TGF-β antagonist attenuates fibrosis but not luminal narrowing in experimental tracheal stenosis

Juan L. Antón-Pacheco[1†], MD; Alicia Usategui[2†], PhD; Iván Martínez[3], MD; Carmen M. García-Herrero[2], PhD; Antonio P. Gamez[3], MD; Montserrat Grau[4], MSc; Ana M. Martínez[5,6], PhD; José L. Rodríguez-Peralto[7], MD, PhD; José L. Pablos[2,8], MD, PhD.

[1]Servicio de Cirugía Pediátrica, Hospital 12 de Octubre, Madrid (Spain); [2]Grupo de Enfermedades Inflamatorias y Autoinmunes, Instituto de Investigación Hospital 12 de Octubre (Imas12), Universidad Complutense de Madrid (Spain); [3]Servicio de Cirugía Torácica, Hospital 12 de Octubre, Madrid (Spain); [4]Unidad de Animalario y Quirófanos Experimentales, Instituto de Investigación Hospital 12 de Octubre (Imas12), Madrid (Spain); [5]Departamento de Bioquímica y Biología Molecular, Facultad de Medicina, Universidad Complutense de Madrid (Spain), [6]Universidad Francisco de Vitoria, Facultad de Ciencias Sanitarias, Escuela de Farmacia, Madrid (Spain), [7]Servicio de Anatomía Patológica, Hospital 12 de Octubre, Madrid (Spain); [8]Servicio de Reumatología, Hospital 12 de Octubre, Universidad Complutense de Madrid, Madrid (Spain).

Running title: TGF-β antagonist reduces tracheal fibrosis

Funding: This work was supported by the Fondo de Investigación Sanitaria, Instituto de Salud Carlos III (FIS PI12/00646 and PI12/439), co-financed by FEDER (European Regional Development Fund).

Conflict of Interest: None.

Corresponding author: José L. Pablos. Instituto de Investigación Hospital 12 de Octubre, 28041 Madrid (Spain). E-mail: jlpablos@h12o.es. Phone 34-91-77924759.

Abstract

Introduction/Objective: Acquired tracheal stenosis (ATS) is an unusual disease often secondary to prolonged mechanical trauma. ATS pathogenesis involves inflammation and subsequent fibrosis with narrowing of the tracheal lumen. TGF-β represents a pivotal factor in most fibrotic processes and therefore, a potential target in this context. The aim of this study is to analyze the role of TGF-β as a target for anti-fibrotic interventions in tracheal stenosis.

Methods: Human stenotic tracheobronchial tissues from patients with benign airway stenosis and normal controls from pneumonectomy specimens were analyzed. Tracheal stenosis was induced in adult NZ rabbits by a circumferential thermal injury to the mucosa during open surgery and re-anastomosis. Rabbits were treated postoperatively with a peritracheal collagen sponge containing a TGF-β peptide antagonist (p17) or vehicle. Fibrosis was determined by Masson's trichrome staining, and α-SMA$^+$ myofibroblasts, CTGF and p-Smad2/3 expression by immunohistochemistry.

Results: Human and rabbit stenotic tissues showed extensive submucosal fibrosis, characterized by significantly increased α-SMA$^+$ myofibroblasts and CTGF expression. In human stenotic lesions, increased p-Smad2/3$^+$ nuclei were also observed. p17 treatment significantly reduced the fibrotic thickness as well as the density of α-SMA$^+$ myofibroblasts and CTGF$^+$ cells in rabbit stenotic lesions but failed to improve the luminal area.

Conclusion: ATS is characterized by a TGF-β dependent fibrotic process but reduction of the fibrotic component by TGF-β1 antagonist therapy was not sufficient to improve tracheal narrowing, suggesting that fibrosis may not be the main contributor to luminal stenosis.

Keywords: Tracheal stenosis, TGF-β antagonist, animal model

Level of Evidence: N/A

Introduction

Acquired tracheal stenosis (ATS) is an unusual disease which main causes are related to mechanical stress by endotracheal intubation or tracheostomy tubes. Burns, trauma, previous surgery, and infectious or autoimmune inflammatory diseases may also be responsible for ATS[1]. Since the initial experience reported by McDonald and Stocks[2] regarding extended endotracheal intubation as a way of ventilatory support in pre-term neonates, the incidence of airway stenosis in children has increased substantially[3]. A long-standing cuffed endotracheal tube may cause mucosal damage and secondary scarring resulting in ATS. The histologic changes observed in the mucosa include inflammation, granulation tissue formation and fibrosis with subsequent narrowing of the tracheal lumen[4].

The type of treatment to be instituted in a patient with ATS depends on the severity, morphologic type of the lesion, and the etiologic factors. An obstruction of 50% or more of the tracheal lumen is definitely symptomatic and requires surgical or endoscopic therapy. In selected cases, tracheal resection of the stenosis with end to end anastomosis may offer a good and permanent result. Endoscopic procedures, such as balloon dilation, laser photoresection or stenting may be indicated in selected cases. Overall, treatment failure for both surgical and endoscopic treatment may vary between 9% and 43% in different studies, due to severe complications such as anastomotic dehiscence, re-stenosis, airway perforation, bleeding, or tracheo-esophageal fistula[5-7].

The role of medical therapy is less clear. Local treatments with corticoids or mitomycin C have been empirically tried with variable results[8,9]. Therefore, the study of the specific factors involved in the development of granulation tissue and fibrosis

causing ATS may help to identify potential therapeutic targets. Although the precise pathomechanism is not known, a general response to injury or mechanical stress to the respiratory epithelium involves selective release of transforming growth factor-β1 (TGF-β1)[10], one of the key molecular factors involved in fibrogenesis[11,12]. Several cellular and molecular pathways such as M2 macrophage dysregulation or activation of the IL-17 axis may initiate the process leading to excessive fibroproliferative responses, an emerging target for intervention[13,14,15].

TGF-β signals through specific receptors that trigger a specific intracellular signalling cascade, leading to phosphorylation and activation of SMAD proteins. pSmad2/3 form a heteromeric complex with Smad4 and translocate into nucleus where they act as specific transcription factors, initiating normal or pathological scarring responses[16,17]. Therefore pSMAD detection is a surrogate marker for TGF-β activation and response. TGF-β response involves differentiation of stromal cells into high extracellular matrix ECM-secreting myofibroblasts, characterized by smooth muscle cell α-actin (α-SMA) expression[18,19]. TGF-β also induces the expression of connective tissue growth factor (CTGF) gene, a cysteine-rich protein that further enhances the pro-fibrotic effects of TGF-β and that is expressed in most fibrotic conditions[20-22]. Therefore, TGF-β represents a potential therapeutic target in different fibrotic conditions. TGF-β antagonistic antibodies or peptides have shown anti-fibrotic activity in a variety of experimental models of fibrosis[23-27].

Several animal models for ATS secondary to different types of trauma that reproduce the formation of a granulation tissue with subsequent fibrosis and stenosis have been described[28-30]. We aim to identify the participation of TGF-β signalling in the pathologic process of human and experimental ATS and to evaluate the capacity of a TGF-β peptide antagonist to reduce fibrosis and tracheal stenosis in an animal experimental model.

Materials and Methods

Ethics statement

All human and animal procedures were approved by Clinical Research Committee and Animal Care and Use Committee of Hospital 12 de Octubre with protocol reference number PI12/00646, and carried out in accordance with the institutional guidelines.

Patients

Human tracheobronchial tissues were obtained by excision of stenotic lesions during elective therapeutic intervention of 7 pediatric or young adult patients with benign ATS (67% male and mean±SD age 20±7 years [11-28 years old]). Normal tracheobronchial tissues were obtained from 9 pulmonary resection specimens indicated by non-tracheal pathology (78% male and mean±SD age 63±4 years [58-70 years old]).

Animal model

We developed a model of tracheal stenosis in adult New Zealand White rabbits (Granja cunícola San Bernardo, Navarra, Spain). Briefly, an incomplete transverse incision of the trachea was performed under anaesthesia, followed by a circumferential thermal injury to the mucosa with electro-cauterization and suture. At 4 weeks the tracheal segment was excised, fixed in formaldehyde 4% solution and paraffin embedded. In preliminary sequential studies from 2 to 12 weeks after the intervention, the maximal stenosis was observed in rabbits sacrificed at 4 weeks.

To determine the degree of stenosis, the luminal areas at the site of injury and at the first distal non-involved tracheal ring were photographed and the stenotic/normal luminal area ratio calculated using ImageJ software (http://rsb.info.nih.gov/ij).

For the intervention study, a total of forty rabbits were divided into two groups (saline and p17 treatment). In addition, a group of ten rabbits was used as control of the surgical procedure.

Histology and immunohistochemistry

Submucosal fibrosis was evaluated as the maximal thickening of the submucosal collagen stained tissue on Masson's trichrome stained tracheal sections, which was measured using ImageJ software. Tracheas were also stained with Safranin O to assess biochemical and structural integrity of cartilage.

Immunohistochemistry (IHC) was performed on deparaffinised and rehydrated tissues, after microwave heating in 1mM EDTA pH8 for antigen retrieval. Immunoperoxidase labelling was performed with mouse monoclonal anti-α-SMA antibody (1A4 clone, Sigma-Aldrich Química, Madrid, Spain), rabbit polyclonal anti-pSmad2/3 antibody and goat polyclonal L20 anti-CTGF antibodies (Santa Cruz Biotechnology, CA, USA) and developed by diaminobenzidine chromogen (Vector Laboratories, Burlingame, CA, USA). Rabbit and human tissues were stained with α-SMA and CTGF antibodies whereas pSmad2/3 antibody could only specifically recognize pSmad2/3 in human tracheal sections.

Immunostained sections were visualized on a Zeiss Scope.A1 microscope (Zeiss, Jena, Germany), photographed and digitalized using an AxioCam ERc 5S camera and ZEN lite 2012 software. The number of α-SMA and CTGF positive cells per area were determined.

Local treatment with p17 TGF-β antagonist

To confirm the involvement of TGF-β in the rabbit experimental model of tracheal stenosis, a peritracheal collagen sponge containing a peptide antagonist of TGF-β p17 (2mg/ml) or control vehicle (0.9% saline) was sutured around the trachea after anastomosis. p17 is a soluble hydrophilic peptide derived from a phage display peptide library. It is capable of blocking the effects of TGF-β1 both in vitro and in vivo and has demonstrated anti-fibrotic activity across different species[24,31-36]. Four weeks after the surgical procedure, rabbits were sacrificed and tracheas were excised and paraffin embedded for histological studies.

Statistical analysis

Statistical differences were analyzed using Prism software v6.0 (GraphPad Software, San Diego, CA, USA). Quantitative data were analyzed by Mann–Whitney U-test and correlation analysis by Spearman's rank test. P values less than 0.05 were considered significant.

Results

Human tracheal stenotic tissue show features of TGF-β driven fibrosis

To analyze the histopathological changes in the tracheobronchial tissue of patients with benign airway stenosis, we compared stenotic specimens with normal control tracheobronchial tissues. Histological examination confirmed an extensive submucosal fibrotic component, with an enhanced collagen stained area, as well as a variable inflammatory cell infiltration and epithelial hyperplasia in all cases of tracheal stenosis (Fig. 1).

To obtain evidence of TGF-β participation in the human submucosal fibrotic lesions, we analyzed by IHC the expression of several surrogate markers of TGF-β signalling. We first compared the presence of nuclear phosphorylated Smad2/3 (p-Smad2/3) in stenotic versus normal tracheobronchial tissues. In normal control tracheas, p-Smad2/3 positive nuclei were rarely observed, whereas in stenotic tissues a significant increase of p-Smad2/3 positive nuclei was observed in both tracheal epithelial and submucosal cells (Fig. 1).

The expression of the TGF-β inducible pro-fibrotic factor CTGF was also significantly increased in stenotic compared to normal tracheobronchial tissues. Whereas normal trachea showed minimal or absent CTGF immunostaining, an important increase in the number of CTGF expressing cells, most with stromal cell shape, in the submucosal fibrotic connective tissue (Fig. 1).

Finally, the presence of α-SMA$^+$ myofibroblasts was analyzed. In normal tracheobronchial tissues, only vascular and smooth muscle structures showed α-

SMA$^+$ expression. In stenotic tissues, an abundant infiltrate by α-SMA$^+$ cells with stromal shape consistent with myofibroblasts was observed in the submucosal fibrotic area (Fig. 1).

The rabbit model of tracheal stenosis reproduces the human fibrotic process

Rabbit tracheal tissues undergoing surgical procedure showed a progressive luminal stenosis from 2 to 4 weeks that tended to spontaneously decrease at 12 weeks (Supp. Fig. S1). Tracheal stenosis was histologically characterized by a prominent fibrotic response in the submucosa, with a significant thickened collagen stained area by Masson's trichrome (Fig. 2). Safranin O staining showed cartilage damage in stenotic areas, as patchy areas of reduced cartilage thickness and weaker proteoglycan staining (Supp. Fig. S2). In addition, epithelial hyperplasia and an abundant inflammatory infiltrate, mainly composed by mononuclear and mast cells, were evident in the stenotic lesion (Fig. 2). A significant increase in the number of α-SMA$^+$ myofibroblasts and CTGF$^+$ cells per area were also observed in stromal cells of stenotic tracheal tissues compared to control group (Fig. 2).

Effect of TGF-β antagonist on experimental tracheal stenosis

To evaluate the potential contribution of TGF-β to the development of submucosal fibrosis and tracheal stenosis, rabbits were treated with peri-tracheal collagen sponges containing the TGF-β inhibitor p17 peptide or vehicle control. Thirty four of 40 rabbits were analyzed at 4 weeks. The rest were excluded due to early mortality or signs of local infection. To quantify fibrosis, we measured the maximal thickness of the submucosal collagen stained area which was significantly reduced in p17 treated compared to saline treated group (Fig. 3). The densities of α-SMA$^+$ myofibroblasts and CTGF$^+$ cells per mm^2 were significantly reduced by p17 treatment (Fig. 3). Focal areas of reduced proteoglycan staining, and reduced cartilage thickness were similarly observed in p17 and control group (Supp. Fig. S2).

The degree of luminal stenosis was evaluated in both groups of rabbits as the stenotic/normal luminal area ratio. Despite the observed reduction in fibrosis, we did not observe a significant increase in the luminal area in p17 compared to saline-treated group (Fig. 4A and 4B). Since this data suggested that stenosis did not improve as much as the fibrotic component, we analysed the correlation between both variables, the collagen thickness and the luminal area. Although there was a trend to negative correlation between the luminal area and collagen thickness, the correlation coefficient was low (r=0.29) and non-significant (Fig. 4C).

Discussion

The investigation of the mediators involved in the development of the granulation tissue and fibrotic response responsible for the development of ATS is relevant to the identification of targets of pharmacological therapies. Non-specific anti-inflammatory strategies such as glucocorticoids have shown a limited therapeutic impact[5,37] and therefore, more specific therapeutic targets are needed. However, obtaining mechanistic information is being limited by human tissue availability and data from appropriate animal models are also scarce.

Previous studies have identified an important submucosal fibrotic component in stenotic lesions, that may be the end-result of the activation of specific inflammatory pathways[13,14,15]. However, the pathogenic relevance of common pro-fibrotic mediators such as the TGF-β pro-fibrotic pathway had not been addressed. Increased expression of TGF-β and VEGF in stenotic lesions has been described[38-40]. TGF-β could be directly induced by mechanical pressure on the respiratory epithelium as suggested by data in cultured bronchial epithelial cells providing a link between mechanical stress and the inflammatory and stenotic response[38].

Our data confirm that there is an important fibrotic component in tracheal stenotic lesions where all surrogate markers of TGF-β signaling are present (p-Smad, CTGF

and α-SMA). In addition, these features were reproduced in the animal model of tracheal stenosis. After the surgical procedure, rabbit tracheal tissues showed marked submucosal fibrosis accompanied by an increase CTGF expression and α-SMA^{+} myofibroblasts. Therefore, this animal model provides a valid preclinical to test the impact of TGF-β antagonist.

We used a peptide antagonist of TGF-β that has demonstrated its ability to reduce fibrosis across different species, by interfering the binding of TGF-β to its receptors in vivo. p17 has shown potent anti-fibrotic effects by interfering TGFβ1 and β2 activity in a variety of animal models, either by systemic or local application[24,26,27,34-36]. Although local application by direct surgical implantation of collagen sponges containing p17 is not a feasible strategy to treat human stenosis, it guaranteed inhibitor availability in this proof of concept study. Since the release of active peptide to tracheal tissue is difficult to determine, a large excess of p17 was empirically used, considering data from previous local and systemic studies. We assume efficient delivery because it resulted into significant reduction of fibrosis but perhaps higher concentrations could have a higher impact on tracheal stenosis.

Our data provide consistent evidence on the role of TGF-β in the pathogenesis of tracheal fibrosis. p17 showed significant anti-fibrotic effects associated with a decreased expression of α-SMA and CTGF, two processes directly induced by TGF-β. However, the significantly reduced accumulation of fibrotic tissue in tracheal submucosa was not accompanied by an improvement in the luminal tracheal stenosis. This suggests that other components such as inflammation, epithelial hyperplasia, or structural changes such as cartilage damage might contribute to the reduced tracheal lumen and remain unmodified despite anti-TGF-β effects on fibrosis. Indeed, we confirmed a poor and non-significant correlation between the degree of fibrosis and the tracheal luminal area in the rabbit experimental model.

Conclusions

In summary, our data show evidence of the relevance of TGF-β in the pathogenesis of fibrosis in a human and an animal model of ATS but also an insufficient therapeutic effect of a TGF-β blocking strategy, suggesting that the fibrosis is only a partial contributor to the reduction of the tracheal lumen in ATS.

Acknowledgements

We thank Vanessa Miranda for excellent technical assistance and Mª Dolores Blanco for help with study design. This work was supported by the Fondo de Investigación Sanitaria, Instituto de Salud Carlos III (FIS PI12/00646 and PI12/439), co-financed by FEDER (European Regional Development Fund).

Authors' contributions

†JLAP and AU have equally contributed and share first authorship; JLAP, AU and JLP planned the project, analyzed the data, interpreted the results, performed statistical analysis and wrote the manuscript; JLAP, AU, IM, CMGH, MG and APG performed the experimental work; JLRP contributed to tissues processing and analysis; AMM contributed new reagents; all authors reviewed, revised and approved the manuscript for submission.

References

1. Mathisen DJ. Surgery of the trachea. Curr Probl Surg 1998;35:453-542.

2. McDonald IH, Stocks JG. Prolonged Nasotracheal Intubation. A Review of Its Development in a Paediatric Hospital. Br J Anaesth 1965;37:161-173.

3. Cotton RT. The problem of pediatric laryngotracheal stenosis: a clinical and experimental study on the efficacy of autogenous cartilaginous grafts placed between the vertically divided halves of the posterior lamina of the cricoid cartilage. Laryngoscope 1991;101:1-34.

4. Minnigerode B, Richter HG. Pathophysiology of subglottic tracheal stenosis in childhood. Prog Pediatr Surg 1987;21:1-7.

5. Grillo HC, Donahue DM, Mathisen DJ, Wain JC, Wright CD. Postintubation tracheal stenosis. Treatment and results. J Thorac Cardiovasc Surg 1995;109:486-492.

6. Mehta AC, Lee FY, Cordasco EM, Kirby T, Eliachar I, De Boer G. Concentric tracheal and subglottic stenosis. Management using the Nd-YAG laser for mucosal sparing followed by gentle dilatation. Chest 1993;104:673-677.

7. Wrigh CD, Grillo HC, Wain JC, et al. Anastomotic complications after tracheal resection: prognostic factors and management. J Thorac Cardiovasc Surg 2004;128:731-739.

8. Daher P, Riachy E, Georges B, Georges D, Adib M. Topical application of mitomycin C in the treatment of esophageal and tracheobronchial stricture: a report of 2 cases. J Pediatr Surg 2007;42:E9-E11.

9. Rahbar R, Jones DT, Nuss RC, et al. The role of mitomycin in the prevention and treatment of scar formation in the pediatric aerodigestive tract: friend or foe? Arch Otolaryngol Head Neck Surg 2002;128:401-406.

10. Tschumperlin DJ, Shively JD, Kikuchi T, Drazen JM. Mechanical stress triggers selective release of fibrotic mediators from bronchial epithelium. Am J Respir Cell Mol Biol 2003;28:142-149.

11. Leask A, Abraham DJ. TGF-beta signaling and the fibrotic response. FASEB J 2004;18:816-827.

12. Roberts AB, Sporn MB, Assoian RK, et al. Transforming growth factor type beta: rapid induction of fibrosis and angiogenesis in vivo and stimulation of collagen formation in vitro. Proc Natl Acad Sci U S A 1986;83:4167-4171.

13. Hillel AT, Samad I, Ma G, et al. Dysregulated macrophages are present in bleomycin-induced murine laryngotracheal stenosis. Otolaryngol Head Neck Surg 2015;153:244-250.

14. Gelbard A, Katsantonis NG, Mizuta M, et al. Idiopathic Subglottic Stenosis is Associated with Activation of the Inflammatory IL-17A/IL-23 Axis. Laryngoscope 2016;doi: 10.1002/lary.26098. [Epub ahead of print].

15. Namba DR, Ma G, Samad I, et al. Rapamycin Inhibits Human Laryngotracheal Stenosis–derived Fibroblast Proliferation, Metabolism, and Function in Vitro. Otolaryngol Head Neck Surg 2015;152:881-888.

16. Massagué J. TGFβ signalling in context. Nat Rev Mol Cell Biol 2012;13:616-630.

17. Prud'homme GJ. Pathobiology of transforming growth factor beta in cancer, fibrosis and immunologic disease and therapeutic considerations. Lab Invest 2007;87:1077-1091.

18. Desmouliere A, Chaponnier C, Gabbiani G. Tissue repair, contraction, and the myofibroblast. Wound Repair Regen 2005;13:7-12.

19. Piera-Velazquez S, Mendoza FA, Jimenez SA. Endothelial to Mesenchymal Transition (EndoMT) in the Pathogenesis of Human Fibrotic Diseases. J Clin Med 2016;5:45.

20. Frazier K, Williams S, Kothapalli D, Klapper H, Grotendorst GR. Stimulation of fibroblast cell growth, matrix production, and granulation tissue formation by connective tissue growth factor. J Invest Dermatol 1996;107:404-411.

21. Igarashi A, Okochi H, Bradham DM, Grotendorst GR. Regulation of connective tissue growth factor gene expression in human skin fibroblasts and during wound repair. Moll Biol Cell 1993;4:637-645.

22. Shi-Wen X, Leask A, Abraham D. Regulation and function of connective tissue growth factor/CCN2 in tissue repair, scarring and fibrosis Cytokine Growth Factor Rev 2008;19:133-144.

23. Santiago B, Gutierrez-Canas I, Dotor J, et al. Topical application of a peptide inhibitor of transforming growth factor-beta1 ameliorates bleomycin-induced skin fibrosis. J Invest Dermatol 2005;125:450-455.

24. Arribillaga L, Dotor J, Basagoiti M, et al. Therapeutic effect of a peptide inhibitor of TGF-beta on pulmonary fibrosis. Cytokine 2011;53:327-333.

25. Ezquerro I J, Lasarte JJ, Dotor J, et al. A synthetic peptide from transforming growth factor beta type III receptor inhibits liver fibrogenesis in rats with carbon tetrachloride liver injury. Cytokine 2003;22:12-20.

26. Murillo-Cuesta S, Rodríguez-de la Rosa L, Contreras J, et al. Transforming growth factor β1 inhibition protects from noise-induced hearing loss. Front Aging Neurosci 2015;20:7-32.

27. Loureiro J, Aguilera A, Selgas R et al. Blocking TGF-β1 protects the peritoneal membrane from dialysate-induced damage. J Am Soc Nephrol 2011;22:1682-1695.

28. Eliashar R, Eliachar I, Gramlich T, Esclamado R, Strome M. Improved canine model for laryngotracheal stenosis. Otolaryngol Head Neck Surg 2000;122:84-90.

29. Nakagishi Y, Morimoto Y, Fujita M, Ozeki Y, Maehara T, Kikuchi M. Rabbit model of airway stenosis induced by scraping of the tracheal mucosa. Laryngoscope 2005;115:1087-1092.

30. Roh JL, Lee YW, Park HT. Subglottic wound healing in a new rabbit model of acquired subglottic stenosis. Ann Otol Rhinol Laryngol 2006;115:611-616.

31. Dotor J, Lopez-Vazquez AB, Lasarte JJ, et al. Identification of peptide inhibitors of transforming growth factor beta 1 using a phage-displayed peptide library. Cytokine 2007;39:106-115.

32. Gil-Guerrero L, Dotor J, Huibregtse IL, et al. In vitro and in vivo down-regulation of regulatory T cell activity with a peptide inhibitor of TGF-beta1. J Immunol 2008;181:126-135.

33. Gonzalo-Gil E, Criado G, Santiago B, Dotor J, Pablos JL, Galindo M. Transforming growth factor (TGF)-β signalling is increased in rheumatoid synovium but TGF-β blockade does not modify experimental arthritis. Clin Exp Immunol 2013;174:245-255.

34. Zarranz-Ventura J, Fernández-Robredo P, Recalde S, et al. Transforming growth factor-beta inhibition reduces progression of early choroidal neovascularization lesions in rats: P17 and P144 peptides. PLoS One 2013;8:e65434.

35. Recalde S, Zarranz-Ventura J, Fernández-Robredo P, et al. Transforming growth factor-β inhibition decreases diode laser-induced choroidal neovascularization development in rats: P17 and P144 peptides. Invest Ophthalmol Vis Sci 2011;52:7090-7097.

36. Sevilla P, Vining KV, Dotor J, Rodriguez D, Gil FJ, Aparicio C. Surface immobilization and bioactivity of TGF-β1 inhibitor peptides for bone implant applications. J Biomed Mater Res B Appl Biomater 2016;104:385-394.

37. Antón-Pacheco JL, Cabezalí D, Tejedor R, López M, Luna C, Comas JV, de Miguel E. The role of airway stenting in pediatric tracheobronchial obstruction. Eur J Cardiothorac Surg 2008;33:1069-1075.

38. Lee YC, Hung MH, Liu LY, et al. The roles of transforming growth factor-beta(1) and vascular endothelial growth factor in the tracheal granulation formation. Pulm Pharmacol Ther 2011;24:23-31.

39. Pokharel RP, Maeda K, Yamamoto T, et al. Expression of vascular endothelial growth factor in exuberant tracheal granulation tissue in children. J Pathol 1999;188:82-86.

40. Wen FQ, Liu X, Manda W, et al. TH2 Cytokine-enhanced and TGF-beta-enhanced vascular endothelial growth factor production by cultured human airway smooth muscle cells is attenuated by IFN-gamma and corticosteroids. J Allergy Clin Immunol 2003;111:1307-1318.

Figure legends

Fig. 1. Histopathological and immunohistochemical evaluation of human tracheal tissues. Representative images of Masson's trichrome and quantitative analysis of p-Smad2/3, CTGF and α-SMA staining in control and stenotic tracheal tissues (Mean±SEM; *p<0.05, **p<0.01, ***p<0.001). Bar 100 μm in Masson's and α-SMA panels and 50 μm in p-Smad2/3 and CTGF panels.

Fig. 2. Histopathological and immunohistochemical evaluation of experimental airway stenosis model in rabbits. Representative images of rabbit control and stenotic trachea at 4 weeks after thermal injury with 25x magnification and insets with 200x magnification (Masson's trichrome). Immunolabeling of α-SMA and CTGF positive cells in control and stenotic tracheal rings in an animal model of airway stenosis. Quantification of tracheal thicknening and α-SMA and CTGF positive cells per area (Data shown are mean±SEM; **p<0.01). Bars 400 μm (25x Masson's panels) and 50 μm (Masson's insets, α-SMA and CTGF staining).

Fig. 3. Effect of p17 treatment on submucosal fibrosis and myofibroblasts and CTGF expression in rabbit experimental model. Rabbits were intraoperatively treated with p17 TGF-β antagonist or saline. Tracheal fibrosis was determined as the collagen area stained by Masson's trichrome, and by the direct measure of tracheal thicknening (upper panel). Representative images and quantification of α-SMA (middle panel) and CTGF (lower panel) positive cells per area. Bar 100 μm, insets bar 25 μm. (Data shown are mean±SEM; **p<0.01, ***p<0.001).

Fig. 4. Luminal stenosis in p17-treated rabbits. Representative images of saline-treated and p17-treated tracheas (A). Cross-section of control (right) and stenotic (left) trachea. Quantitative analysis of tracheal luminal area in saline or p17 treated

rabbits (B). Correlation analysis between the luminal area and collagen thicknening (C).

Supp. Fig. S1. Macroscopic analysis of rabbit tracheal sections undergoing surgical procedure. Images show the area of maximal luminal stenosis (left rings) compared with the first distal uninvolved ring (right rings), at the indicated time points after surgery.

Supp. Fig. S2. Evaluation of cartilage structure and proteoglycan staining in rabbit tracheal tissues. Representative images of cartilage damage determined by safranina O stained area in control (left), saline (middle) and p17-treated rabbits (right) are shown. Bar 100 µm.

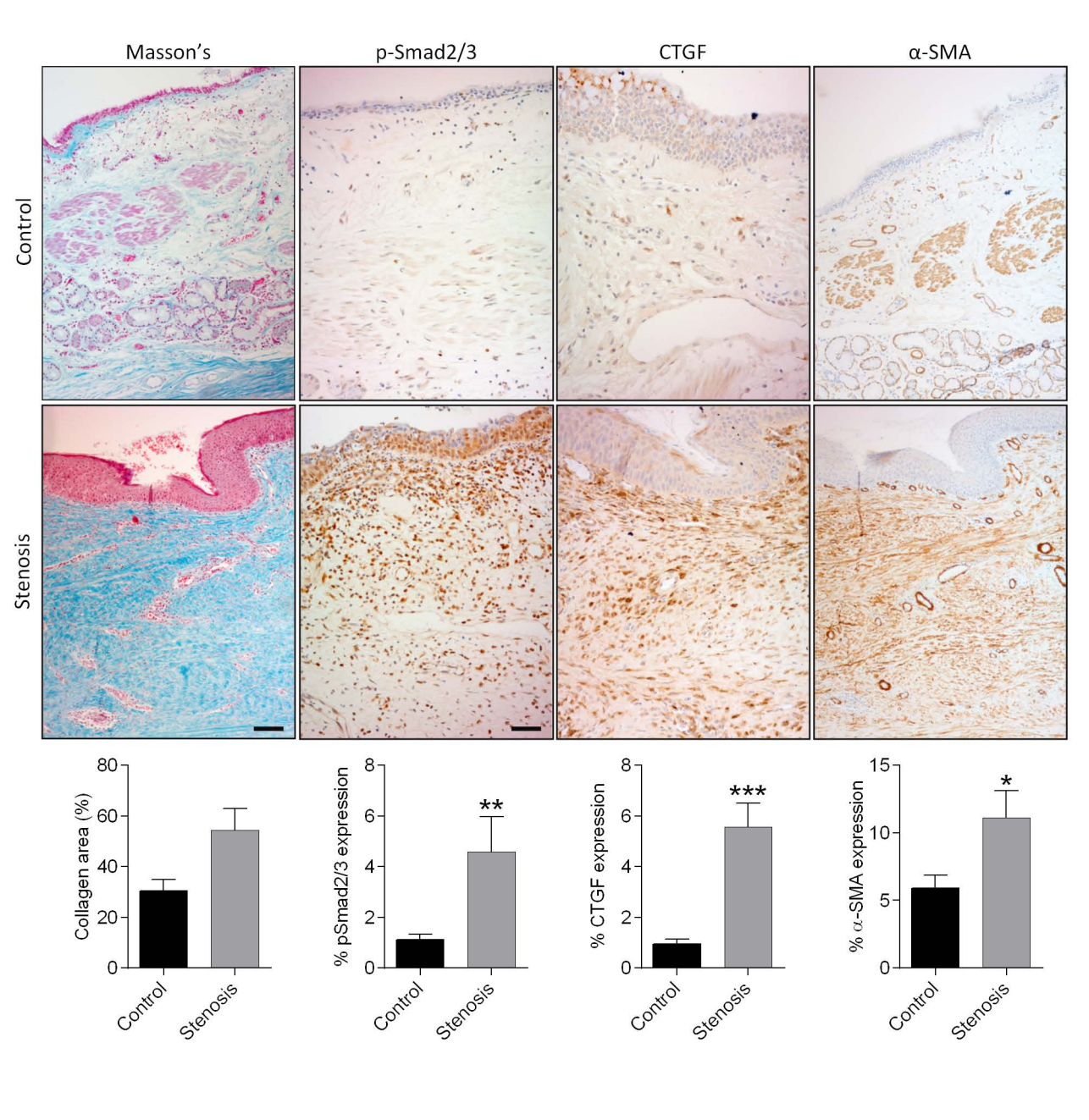
Masson's
p-Smad2/3
CTGF
α-SMA
Control
Stenosis
Collagen area (%)
0
20
40
60
80
Control
Stenosis
% pSmad2/3 expression
0
2
4
6
8
**
Control
Stenosis
% CTGF expression
0
2
4
6
8
***
Control
Stenosis
% α-SMA expression
0
5
10
15
*
Control
Stenosis

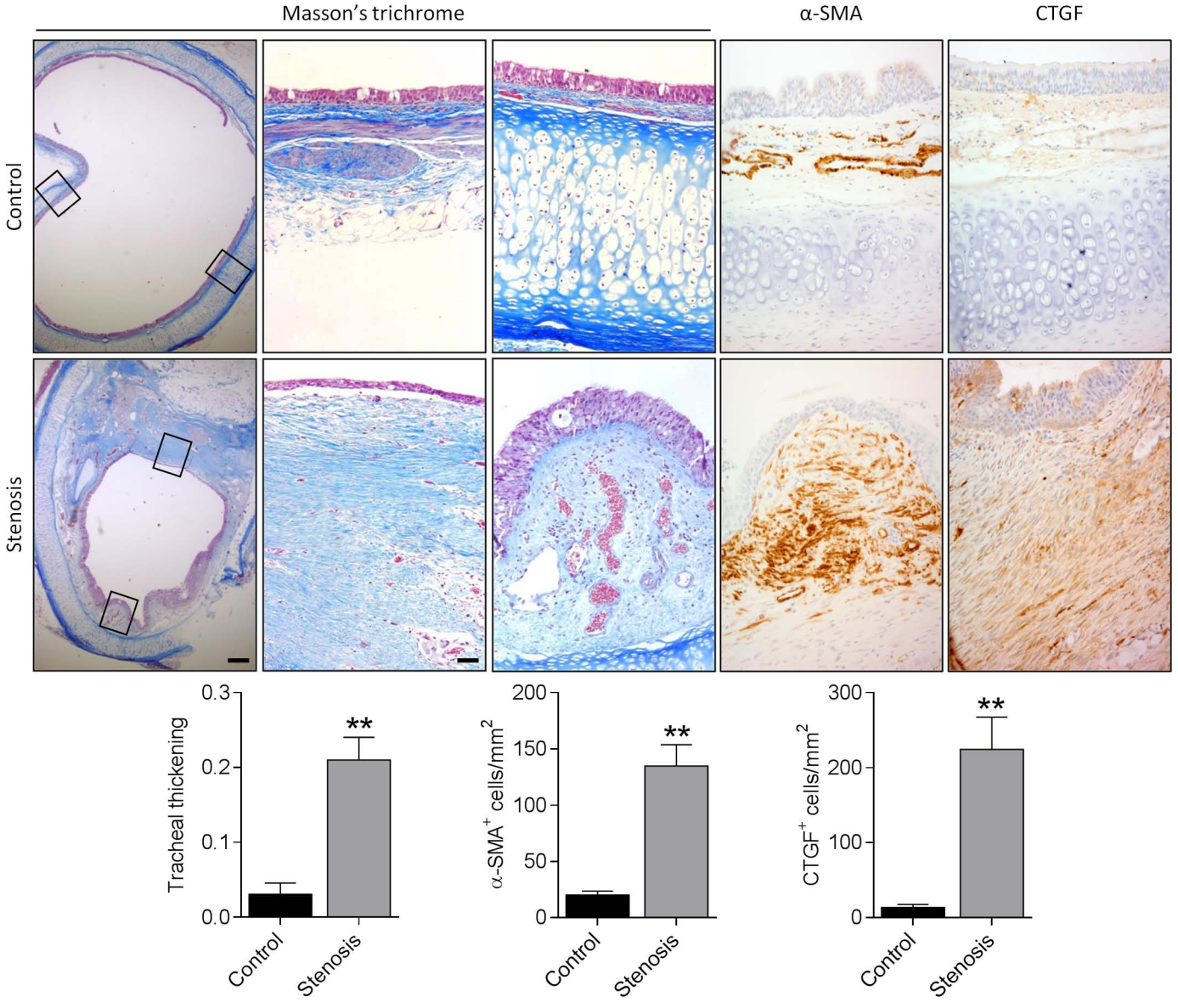
Masson's trichrome
α-SMA
CTGF
Control
Stenosis
Tracheal thickening
0.3
0.2
0.1
0.0
**
Control
Stenosis
α-SMA+ cells/mm2
200
150
100
50
0
**
Control
Stenosis
CTGF+ cells/mm2
300
200
100
0
**
Control
Stenosis

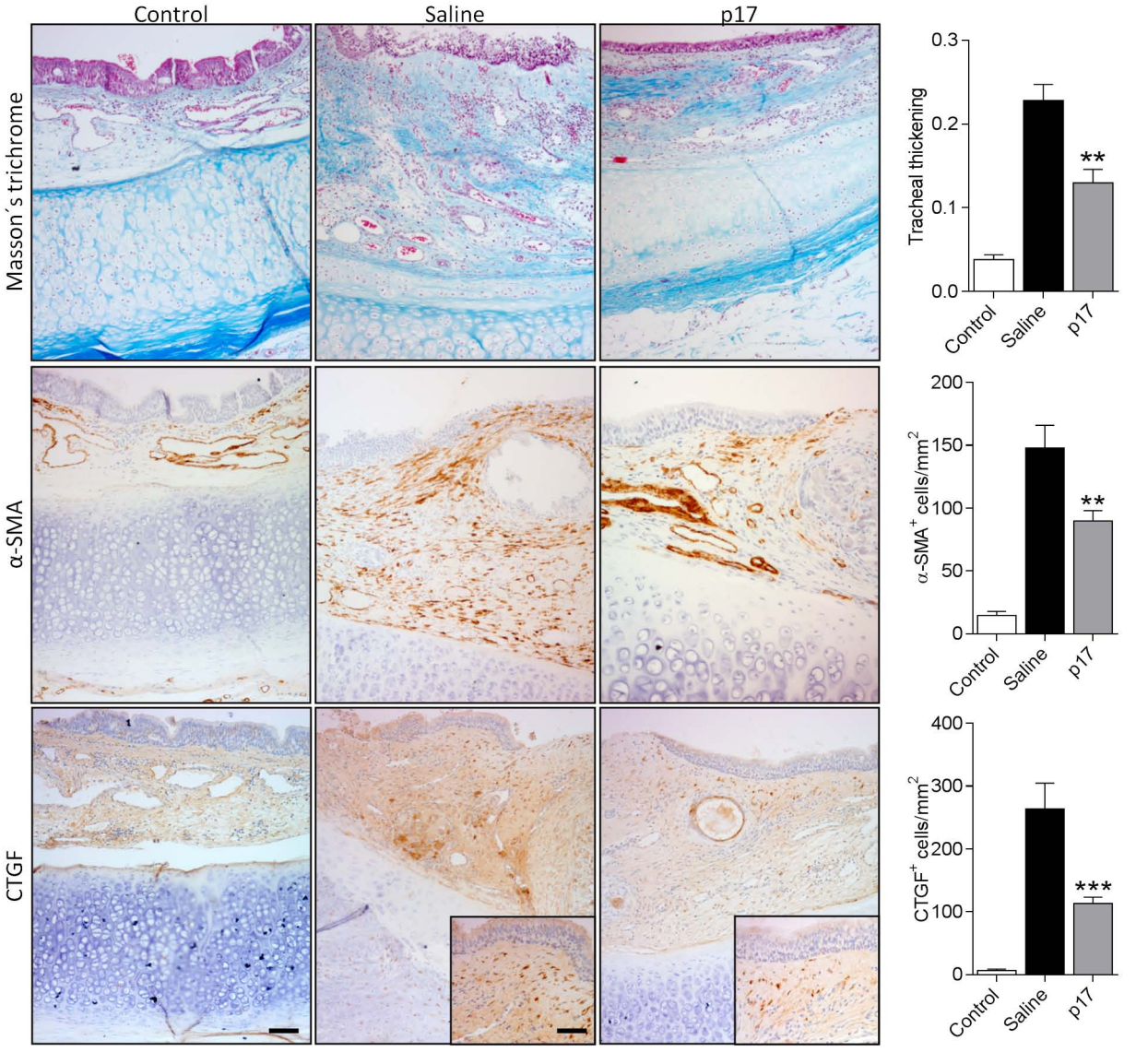
Control
Saline
p17
Masson´s trichrome
α-SMA
CTGF
Tracheal thickening
0.3
0.2
0.1
0.0
**
Control
Saline
p17
α-SMA+ cells/mm2
200
150
100
50
0
**
Control
Saline
p17
CTGF+ cells/mm2
400
300
200
100
0
***
Control
Saline
p17

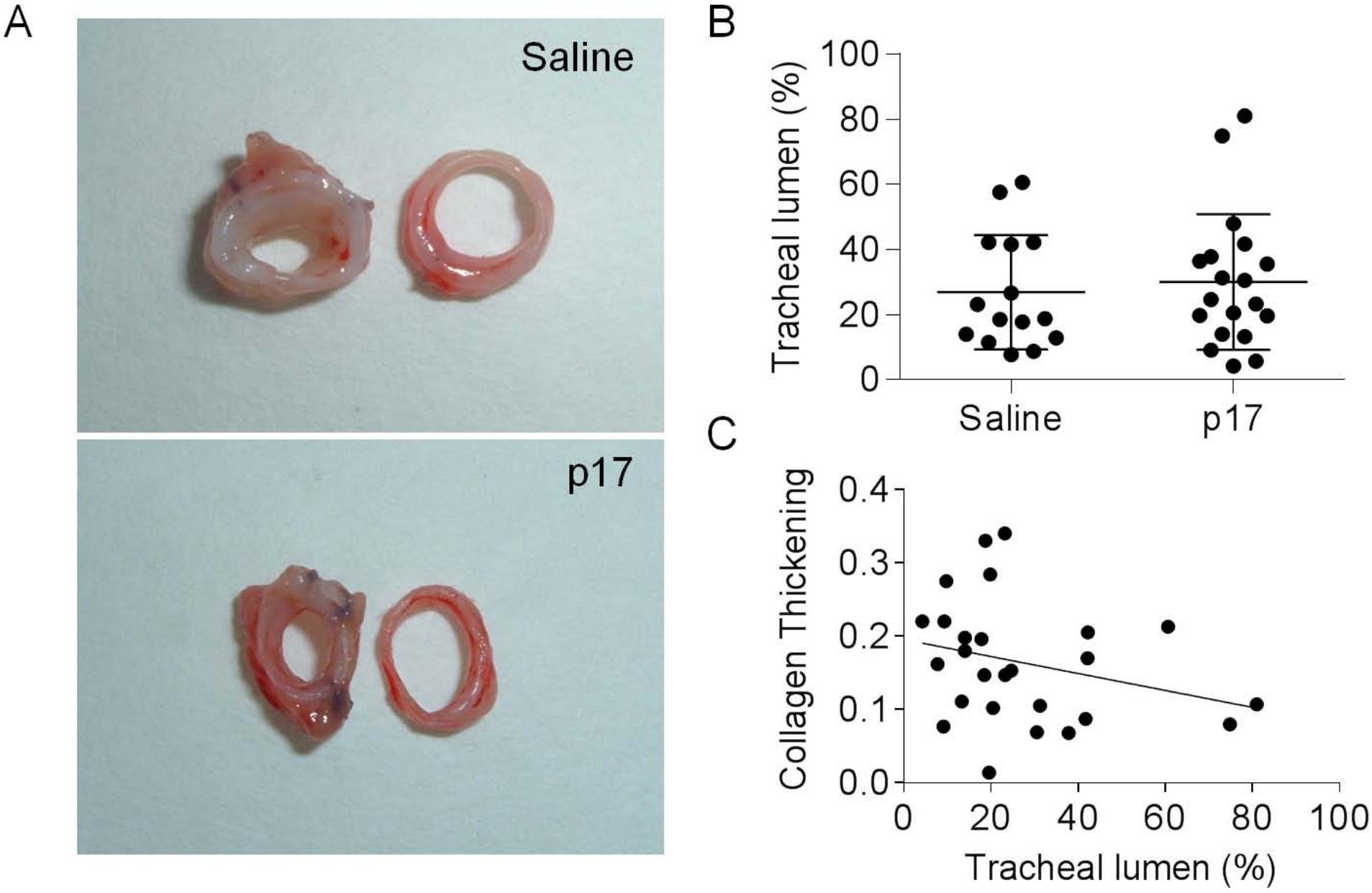
A
Saline
p17
B
Tracheal lumen (%)
100
80
60
40
20
0
Saline
p17
C
Collagen Thickening
0.4
0.3
0.2
0.1
0.0
0
20
40
60
80
100
Tracheal lumen (%)

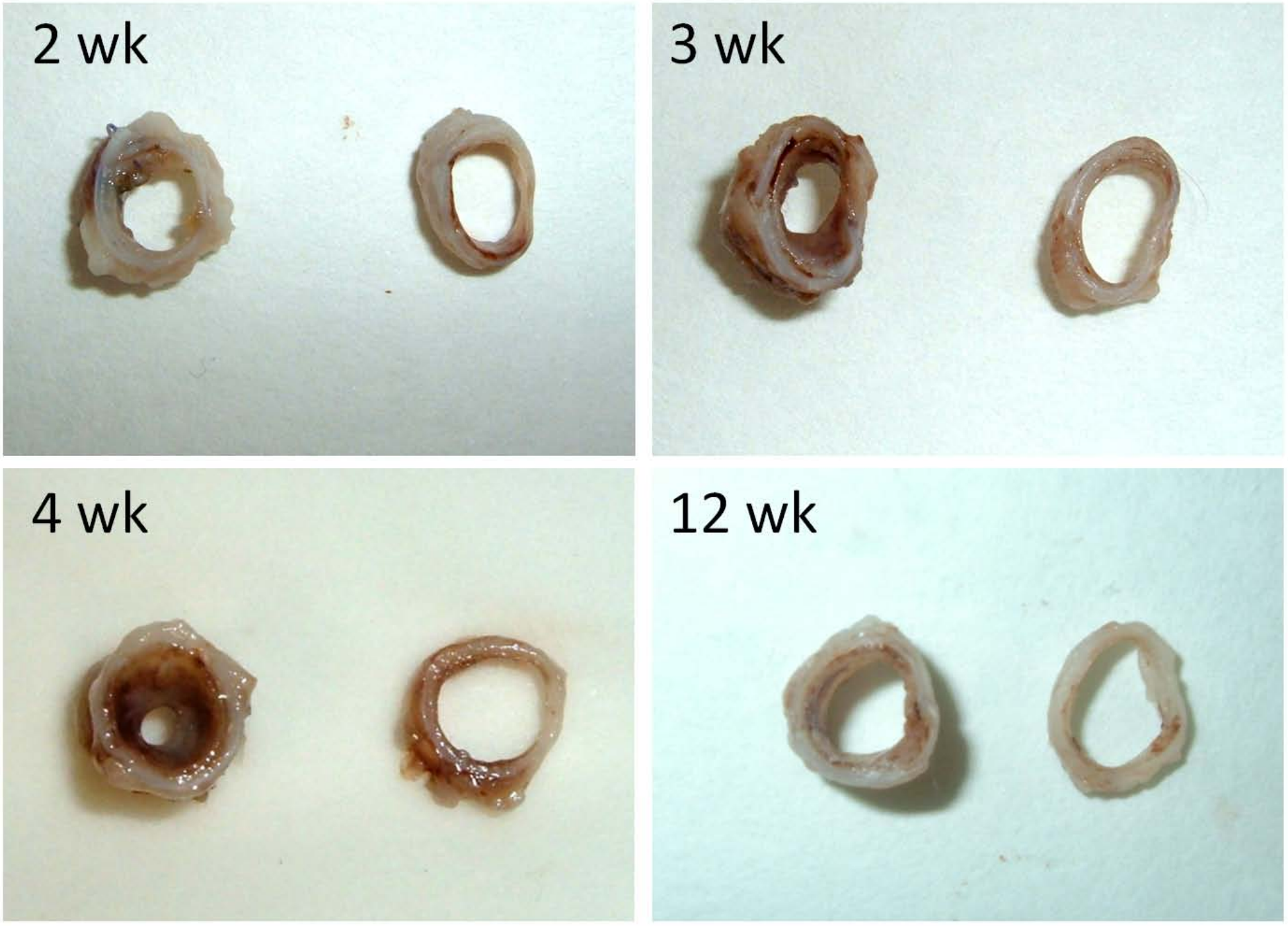
2 wk
3 wk
4 wk
12 wk

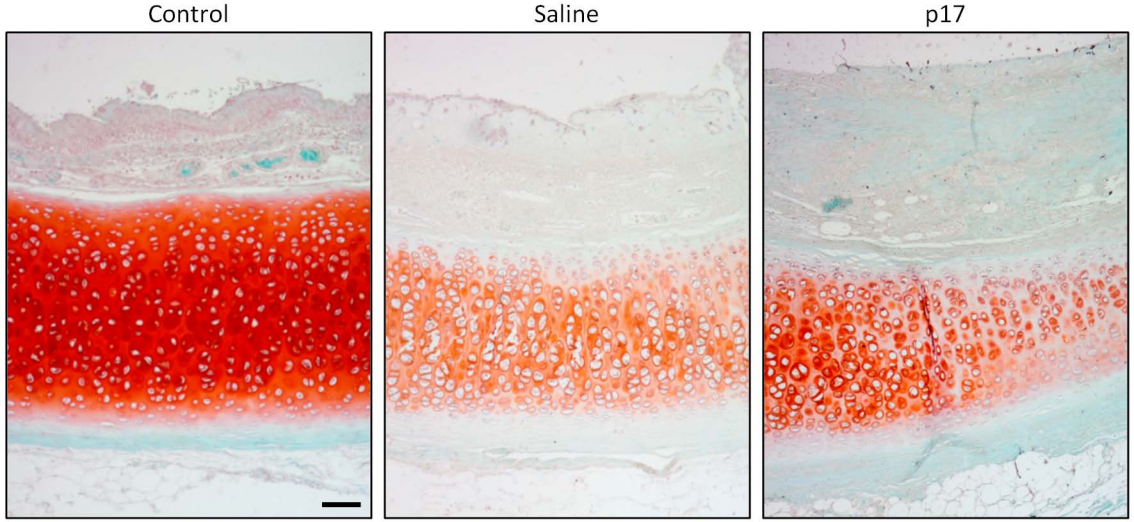
Control
Saline
p17